The PTEN and INK4A/ARF tumor suppressors maintain myelolymphoid homeostasis and cooperate to constrain histiocytic sarcoma development in humans

Daniel R. Carrasco,[1,3] Tim Fenton,[2] Kumar Sukhdeo,[1] Marina Protopopova,[1,4] Miriam Enos,[1] Mingjian J. You,[3] Dolores Divicio,[1] Cristina Nogueira,[1] Jayne Stommel,[1] Geraldine S. Pinkus,[3] Christopher Fletcher,[3] Jason L. Hornick,[3] Webster K. Cavenee,[2] Frank B. Furnari,[2] and Ronald A. DePinho[1,4,*]

[1] Department of Medical Oncology, Dana-Farber Cancer Institute and Harvard Medical School, Boston, Massachusetts 02115
[2] Ludwig Institute for Cancer Research, University of California, San Diego, School of Medicine, La Jolla, California 92093
[3] Department of Pathology, Brigham and Women's Hospital, Harvard Medical School, Boston, Massachusetts 02115
[4] Center for Applied Cancer Science, Belfer Foundation Institute for Innovative Cancer Science, Dana-Farber Cancer Institute, Harvard Medical School, Boston, Massachusetts 02115
*Correspondence: ron_depinho@dfci.harvard.edu

Summary

Histiocytic sarcoma (HS) is a rare malignant proliferation of histiocytes of uncertain molecular pathogenesis. Here, genetic analysis of coincident loss of *Pten* and *Ink4a/Arf* tumor suppressors in the mouse revealed a neoplastic phenotype dominated by a premalignant expansion of biphenotypic myelolymphoid cells followed by the development of HS. Pten protein loss occurred only in the histiocytic portion of tumors, suggesting a stepwise genetic inactivation in the generation of HS. Similarly, human HS showed genetic or epigenetic inactivation of PTEN, $p16^{INK4A}$, and $p14^{ARF}$, supporting the relevance of this genetically engineered mouse model of HS. These genetic and translational observations establish a cooperative role of *Pten* and *Ink4a/Arf* in the development of HS and provide mechanistic insights into the pathogenesis of human HS.

Introduction

The *PTEN* tumor suppressor gene is mutated in diverse human cancers including glioblastoma, prostate cancer, endometrial cancer, breast cancer, and anaplastic meningiomas (Li et al., 1997; Steck et al., 1997). Mutations in *PTEN* are also frequently encountered in primary leukemias and lymphomas (Sakai et al., 1998) and are thought to contribute to tumor initiation and/or progression in the lymphoid compartment. The *PTEN* gene encodes a dual-specificity phosphatase, whose major substrate is phosphatidyl inositol-3,4,5-triphosphate (PIP3), a second messenger molecule produced by PI3K activation following growth factor stimulation. PIP3 in turn activates the serine-threonine kinase PKB/AKT, a positive regulator of cell survival, proliferation, and oncogenesis (Cantley and Neel, 1999; Simpson and Parsons, 2001). Thus, the dephosphorylation of PIP3 by PTEN leads to decreased cell survival.

In the mouse, *Pten* nullizygosity leads to early embryonic lethality, whereas *Pten* heterozygosity results in lymphoid hyperplasia, T cell lymphomas, and endometrial, prostatic, and breast cancers (Di Cristofano et al., 1998; Podsypanina et al., 1999; Suzuki et al., 1998). Pten appears to play a particularly prominent role in growth regulation of immunocytes, as evidenced by the prevalence of autoimmune disorders in $Pten^{+/-}$ mice (Di Cristofano et al., 1999). Similarly, T cell-specific ablation of a conditional *Pten* null allele leads to the development of $CD4^+$ lymphomas and autoimmunity, the latter relating to impaired thymic negative selection and peripheral tolerance (Suzuki et al., 2001). In contrast, B cell-specific deletion of a conditional *Pten* null allele impairs B cell homeostasis and immunoglobulin class switch recombination, but does not provoke the development of B cell lymphomas (Suzuki et al., 2003). Outside the hematopoietic system, there is experimental evidence that *Pten* actively maintains the balance between different cell types in the adult pancreas and that misregulation of the PI3K pathway in centroacinar cells may contribute to the initiation of pancreatic carcinoma in vivo. (Stanger et al., 2005).

The overlapping reading frames in the *INK4A/ARF* locus encode two distinct tumor suppressors, $p16^{INK4A}$ and $p14^{ARF}$ ($p19^{ARF}$ in mice) that function as regulators of the pRB and p53 pathways, respectively (Quelle et al., 1995; Sharpless and DePinho, 1999). $p16^{INK4A}$ and other members of the INK4A

SIGNIFICANCE

HS in humans is a rare malignancy that is typically very aggressive and poorly responsive to existing therapy. As the molecular etiology of this neoplasm is not known, the development and deployment of rational targeted therapeutics have not been possible. Progress in this area has also been hampered by a paucity of biological systems (cellular and organismal) that can validate suspected target genes. Here, we provide genetic evidence of the cooperative interactions of the PTEN and INK4A/ARF tumor suppressor genes in the development of human and mouse HS. Therefore, $Pten^{+/-}$ $Ink4a/Arf^{-/-}$ double mutant mice constitute a model system ideal for dissecting HS pathogenesis and for testing PI3K and cdk4/6 targeted agents in this currently intractable disease.

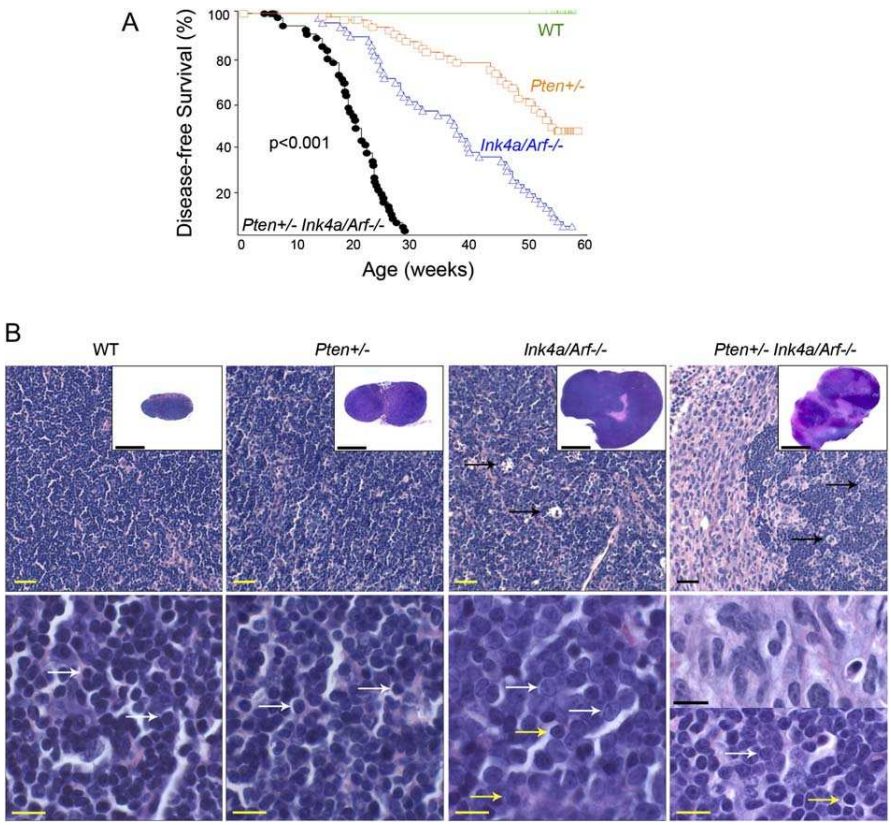

Figure 1. HS in *Pten*$^{+/-}$ *Ink4a/Arf*$^{-/-}$ mice

A: Disease-free survival analysis of wild-type (WT), *Pten*$^{+/-}$, *Ink4a/Arf*$^{-/-}$, and *Pten*$^{+/-}$ *Ink4a/Arf*$^{-/-}$ mutant mice. Statistically significant differences for pairwise comparison ($p < 0.001$) were detected between cohorts.

B: Low-power photomicrographs (inserts) and representative H&E-stained sections from WT, *Pten*$^{+/-}$, *Ink4a/Arf*$^{-/-}$, and *Pten*$^{+/-}$ *Ink4a/Arf*$^{-/-}$ lymph nodes are shown. Arrows: tingible body macrophages (black), reactive lymphocytes (yellow). Scale bars: upper panels, 50 μm; lower panels, 20 μm; inserts, 0.5 cm.

family inhibit G1 cyclin D-dependent kinases 4 and 6, thereby preventing CDK4/6-directed pRB hyperphosphorylation and blocking S phase entry. p14^{ARF} inhibits MDM2-mediated degradation of p53 and plays an important role in the apoptotic elimination of aberrantly cycling cells (Quelle et al., 1995; Sharpless and DePinho, 1999). A wide spectrum of human cancer types exhibit INK4A/ARF inactivation, including malignant glioma, melanoma, and non-Hodgkin's lymphoma (Burri et al., 2001; Ruas and Peters, 1998; Sharpless and DePinho, 1999).

In the mouse, an extensive analysis of p16^{INK4a} and p19^{ARF} has revealed their key roles in the hematopoietic system. Mice carrying a targeted deletion of the *Ink4a/Arf* locus that eliminates both the p16^{INK4a} and p19^{ARF} proteins succumb to B cell lymphomas and malignant spindle cell neoplasms (Serrano et al., 1996). Mice lacking p19^{ARF}, yet intact for p16^{INK4a}, develop predominantly T cell lymphomas (Kamijo et al., 1997). Similarly, *p16*^{Ink4a}-specific knockout mice show increased incidence of spontaneous and carcinogen-induced cancers including soft-tissue sarcomas, melanoma, and splenic histiocytic lymphomas (Krimpenfort et al., 2001; Sharpless et al., 2001), thereby demonstrating that both gene products encoded by this locus exert important and nonoverlapping tumor suppressor roles in diverse lineages. Of special relevance to this report, both p16^{INK4a} and p19^{ARF} have been shown to constrain immortalization of bone marrow-derived macrophages (Randle et al., 2001). Finally, increasing *Ink4a/Arf* mRNA expression is a biomarker of aging tissues including lymphoid cells (Krishnamurthy et al., 2004) and may engender the loss of hematopoietic stem cells during proliferative stress as evaluated by serial transplantation of *Ink4a/Arf*$^{-/-}$ HSCs in mice (Stepanova and Sorrentino, 2005). Overall, the role and regulation of the p16^{INK4a} and p19^{ARF} in the hematopoietic system and their interactions with other cancer-relevant pathways continues to be an area of active investigation.

HS is a rare malignant proliferation of neoplastic cells showing immunophenotypic and morphologic features similar to histiocytes (tissue macrophages) that occurs in lymph nodes, skin, and the gastrointestinal tract and it is of unknown etiology. It is now recognized that most cases of HS described in the past actually represented diffuse/anaplastic large B cell lymphoma, peripheral T cell lymphoma associated with hemophagocytic syndrome, or lymphoma with associated reactive macrophages. Only small numbers of bona fide examples exist in the world literature (Weiss, 2001). Here, we report the functional consequences of *Pten* and *Ink4a/Arf* mutations in normal development and neoplasia of the murine hematopoietic system and provide mechanistic insights into the pathogenesis of human HS.

Results

Impact of *Pten* and *Ink4a/Arf* tumor suppressor mutations on the lymphoid and histiocytic compartments

Pten$^{+/-}$ *Ink4a/Arf*$^{+/-}$ mice were intercrossed to generate cohorts of wild-type, *Pten*$^{+/-}$, *Ink4a/Arf*$^{-/-}$, and *Pten*$^{+/-}$ *Ink4a/Arf*$^{-/-}$ mice that were monitored closely for perturbations in the lymphoid system. Consistent with previous reports, *Pten*$^{+/-}$ and *Ink4a/Arf*$^{-/-}$ littermates had a mean disease-free survival (lack of palpable adenopathy) that averaged 52 and 29 weeks, respectively (Cline, 1994), while *Pten*$^{+/-}$ *Ink4a/Arf*$^{-/-}$ mice succumbed between 10 and 32 weeks (mean 19 weeks; $p < 0.001$) to a rapidly progressive disease characterized by generalized wasting and enlarged lymph nodes (Figure 1).

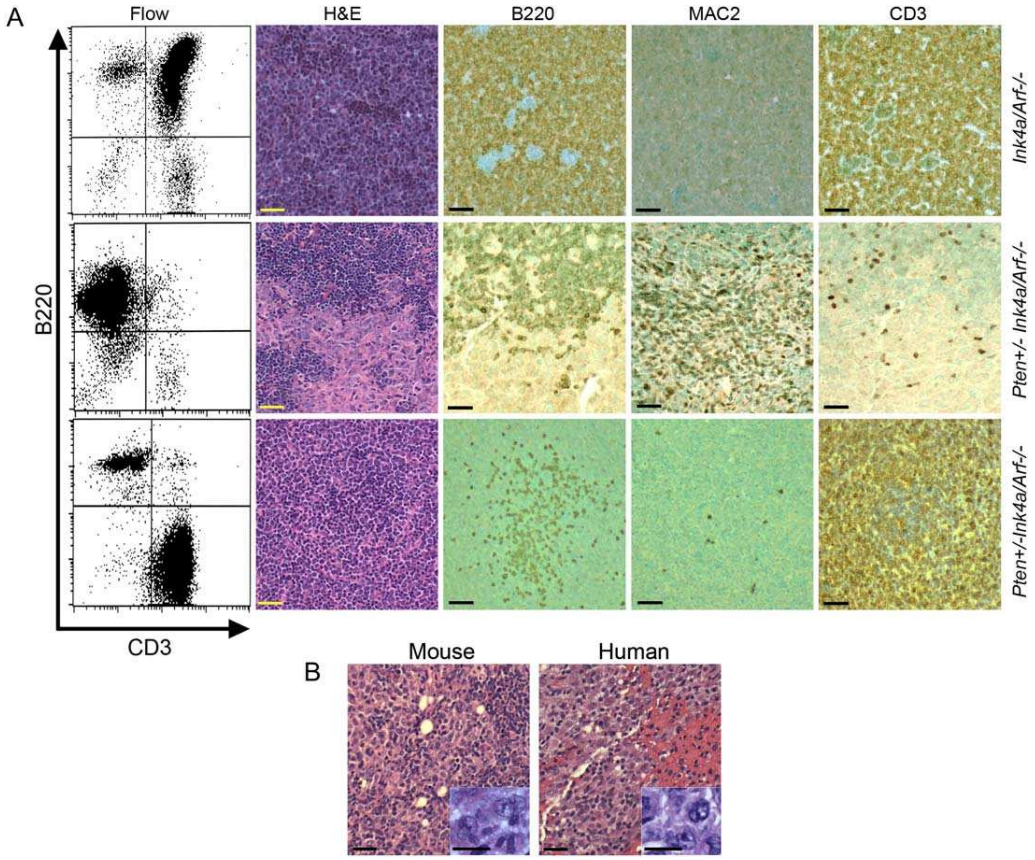

Figure 2. Immunophenotype of lymphomas and HS

A: Representative tumor types arising from *Ink4a/Arf*$^{-/-}$ or *Pten*$^{+/-}$ *Ink4a/Arf*$^{-/-}$ mice were analyzed by flow cytometry, H&E staining, and immunohistochemistry for B220, MAC2, and CD3 antibodies. The upper panel represents a biphenotypic LL (B220^{+}, MAC2^{-}, CD3^{+}). The middle panel represents a composite lymphoma bearing areas of B cell LL (upper portion, dark blue areas; B220^{+}, MAC2^{-}, CD3^{-}) and areas of HS (lower portion, pink light areas; B220^{-}, MAC2^{+}, CD3^{-}). The lower panel represents a case of T LL (B220^{-}, MAC2^{-}, CD3^{+}).

B: Morphologic resemblance between *Pten*$^{+/-}$ *Ink4a/Arf*$^{-/-}$ mouse and human HS as seen by comparing representative examples of *Pten*$^{+/-}$ *Ink4a/Arf*$^{-/-}$ mouse HS (left) and human HS (right) are shown. Scale bars: 50 μm; inserts, 20 μm.

While all mutant animals developed enlarged lymphoid tissues, there were marked differences in lymphoid tumor histology among the various mutant genotypes. *Pten*$^{+/-}$ mice showed lymphoid hyperplasia with some nodal architectural distortion, but not effacement of normal lymphoid architecture (Figure 1B). In agreement with these benign histological features, B and T cell receptor gene rearrangement analyses revealed polyclonal/oligoclonal patterns in 30 of 31 cases examined over a 1 year period of observation, and the sole exception was a *Pten*$^{+/-}$ mouse that developed a histological picture of lymphoma with a documented clonal T cell receptor gene rearrangement pattern (Table 1 and Figure S1A in the Supplemental Data available with this article online, lane 6). *Ink4a/Arf*$^{-/-}$ mice showed replacement of the normal lymph node architecture by a homogeneous population of medium-sized atypical lymphoid cells, and a "starry sky" pattern was evident due to presence of frequent mitotic figures and numerous tingible body macrophages (Figure 1B). According to the Bethesda guidelines for classification of lymphoid neoplasms in mice (Morse et al., 2002), most tumors in *Ink4a/Arf*$^{-/-}$ mice were classified as precursor B or T lymphoblastic lymphoma (LL). Flow cytometric, immunohistochemical (Figure 2A), and gene rearrangement studies revealed that most of the lymphomas were of B cell origin, fewer were of T cell origin, and rarely biphenotypic, i.e., displayed surface marker expression (Figure 2A) and clonal gene rearrangements of both T and B cell lineages (Table 1, Figure 3A, and data not shown). Of the seven T cell lymphomas, one was CD4^{-}CD8^{+}, one was CD4^{+}CD8^{+}, and five were CD4^{+}CD8^{-} (data not shown).

In contrast to the single mutant mice, *Pten*$^{+/-}$ *Ink4a/Arf*$^{-/-}$ mice showed early lymphomatous involvement with a biphasic histological pattern in 30 of 40 mice, consistent with both T or B cell lymphoma and HS. Specifically, we observed dark blue staining areas (Figure 1B) consisting of lymphoblastic cells with phenotypes and genotypes of B cells, T cells, or B and T cells (Figures 2A and 3A). This *Pten*$^{+/-}$ *Ink4a/Arf*$^{-/-}$ lymphoma picture was similar to that described above for the *Ink4a/Arf*$^{-/-}$ mice, including the predominance of B cell over T cell lymphomas (Table 1). However, a notable difference in the *Pten*$^{+/-}$ *Ink4a/Arf*$^{-/-}$ cohort was the presence of light pink areas comprised of very large cells with hyperchromatic, irregular nuclei, clumped chromatin, prominent nucleoli, and abundant eosinophilic cytoplasm (Figures 1 and 2A). These large cells expressed the histiocytic cell markers MAC2 and F4/80 (Figures

Table 1. Lymphoma phenotype/genotype

	Wild-type	*Pten*$^{+/-}$	*Ink4a/Arf*$^{-/-}$	*Pten*$^{+/-}$ *Ink4a/Arf*$^{-/-}$
Normal	30	0	2	0
Lymphoproliferative disorder	0	31	1	3
Lymphoblastic T cell lymphoma	0	1	7	6
Lymphoblastic B cell lymphoma	0	0	24	30*
Biphenotypic B and T cell lymphoma	0	0	2	1
Histiocytic sarcoma	0	0	4	30*
Total	30	31	40	40

*The majority of *Pten*$^{+/-}$*Ink4a/Arf*$^{-/-}$ hematopoietic tumors (30/40) showed a biphasic pattern of both lymphoblastic lymphoma and histiocytic sarcoma.

2A and 3C and data not shown) and were negative for B cell markers (B220 and Bcl-6), for pan-T cell markers (CD3, CD4 [variable] and CD8), and for myeloperoxidase, Gr-1, and Mac-1 (Figures 2A, 3C, and 5A and data not shown). These histological and immunophenotypic features resemble those of human HS (Figure 2B). Only 4 of 40 *Ink4a/Arf*$^{-/-}$ lymphomas (4/40) showed a histiocytic component, and this phenotype was limited primarily to the white pulp areas of the spleen (Table 1). These data clearly demonstrate a change of tumor spectrum brought about by combined *Pten* and *Ink4a/Arf* deficiency and, together with the accelerated onset of disease in compound mutant mice, indicate genetic cooperation between

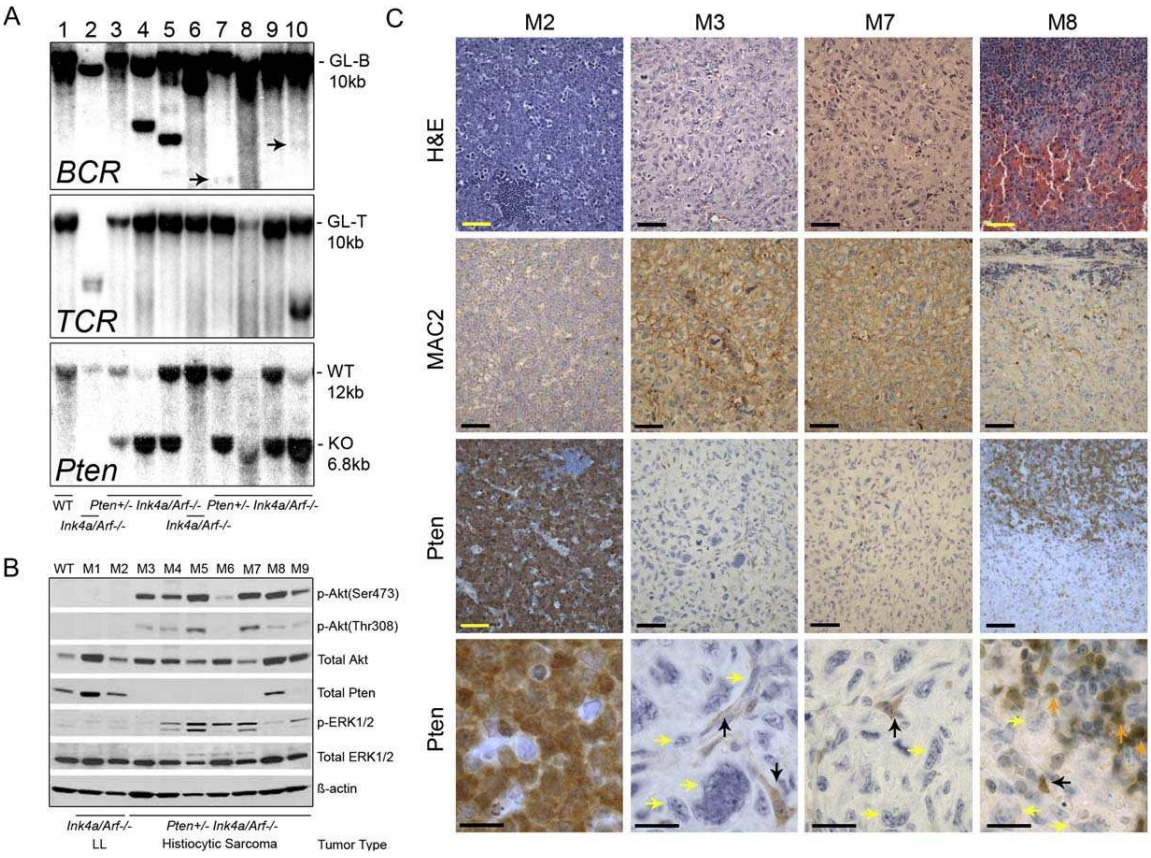

Figure 3. Southern and Western blots of lymphomas and HS

A: Clonal B cell (*BCR*) and T cell (*TCR*) receptor gene rearrangement analysis by Southern blot using DNA isolated from WT (lymph nodes), *Ink4a/Arf*$^{-/-}$ lymphomas (lanes 2 and 6) and *Pten*$^{+/-}$ *Ink4a/Arf*$^{-/-}$ HS cases (lanes 2–4 and 7–9). Arrows indicate small clonal bands in lanes 7 and 10. Germline configuration of the B cell receptor gene (GL-B). Germline configuration of the T cell receptor gene (GL-T). Lanes 2 and 10 show presence of clonal bands for both the B and T cell receptor genes. Southern blot using a probe recognizing WT and knockout forms of the *Pten* locus (*Pten*) to document zygosity. Targeted inactive allele of *Pten* (KO). Note loss of the remaining WT *Pten* allele (lanes 4, 8, and 10).

B: Western blot demonstrating Akt activation in HS from *Pten*$^{+/-}$ *Ink4a/Arf*$^{-/-}$ (samples M3–M9) compared to WT spleen (lane 1) and in LL from *Ink4a/Arf*$^{-/-}$ mice (M1 and M2) by immunoblotting with phospho-specific Akt antibodies to S473 and T308 (see text). ERK1/2 activation was assessed using phospho-specific antibodies to T202/Y204. The approximate tumor cellularity of the HS samples was 90% in M3–M7 and 70%–80% in M8 and M9—estimated by the extent of normal tissue infiltration determined by Pten immunohistochemistry.

C: Pten immunohistochemical analysis in mouse HS. Tissue sections from one case of LL (M2) and three cases of HS were unstained or stained with MAC2 or Pten antibodies. Note preservation of Pten immunoreactivity in M2 (same as Figure 3B) LL and loss of reactivity in HS (M3, M7, M8) (same as Figure 3B). Arrows indicate the following: HS cells (yellow), stroma (black), normal lymphoid cells (orange). Scale bars: 50 μm.

Pten and *Ink4a/Arf* mutations in lymphomagenesis and the development of HS.

Loss of *Pten* and activation of Akt and Erk in HS

Southern blot analysis of the remaining wild-type *Pten* allele in the lymphomas arising in $Pten^{+/-}$ $Ink4a/Arf^{-/-}$ mice revealed wild-type *Pten* gene deletion in 13 of 40 cases (33%) (Figure 3A). The remaining faint wild-type *Pten* band likely represents a minor proportion of nonneoplastic cells as documented by immunohistochemistry with Pten antibodies and argues that *Pten* reduction to homozygosity occurs in both the histiocytic and the lymphoblastic components (see below). Notably, in contrast to tumors arising in $Pten^{+/-}$ $Ink4a/Arf^{-/-}$ mice, 31 of 32 of the lymphoproliferative lesions arising in $Pten^{+/-}$ mice retained the wild-type *Pten* allele, with the sole exception of a lymphoma arising in an aged mouse (Figure S1A, lane 6).

Aberrant activation of the PI3K/Akt signaling pathway, leading to uncontrolled cell growth, proliferation, and survival is well documented in a wide variety of cancers and is thought to be the major mechanism by which loss of Pten promotes tumor progression (Cantley and Neel, 1999). Since the development of HS was seen only in those $Ink4a/Arf^{-/-}$ mice also missing one *Pten* allele, we hypothesized that reduction or loss of Pten function, leading to hyperactivation of Akt signaling, may be an important feature of these tumors. Full activation of Akt is dependent upon phosphorylation of two residues, T308 in the activation loop and S473 in the hydrophobic motif (Vanhaesebroeck and Alessi, 2000). Western blotting with phospho-specific antibodies against both of these residues clearly indicated increased Akt activation in the majority of HS samples, while lymphomas arising in $Ink4a/Arf^{-/-}$ mice show no increase in Akt phosphorylation when compared with normal tissue from wild-type mice (Figure 3B). Examination of Pten levels in these samples (Figure 3B), with a sole exception in sample M8, suggested a loss of Pten protein from the majority of HS samples, which can largely be attributed to loss of heterozygosity in the tumor cells as determined by Southern blot analysis (Figure 3A). These results prompted us to investigate the levels of Pten protein expression in HS samples by immunohistochemistry (Figure 3C). Remarkably, in all samples analyzed, histiocytic tumor cells lacked immunoreactivity for Pten, while stromal cells and some contaminating normal lymphoid cells retained Pten signal (Figure 3C). These results demonstrate that the Pten band seen in sample M8 by Western blot analysis (Figure 3B) is likely due to infiltration of normal cells in this tumor, which accounts for up to 30% of the cellularity in this sample. These results also demonstrate that loss of Pten function is a required mechanism for the development of HS. Interestingly, sample M7 revealed preservation of the wild-type allele by Southern blot analysis (data not shown), indicating that additional mechanisms for Pten loss may operate in some tumor samples. Sequence analysis of *Pten* encoding sequences in HS samples M3–M9 did not detect any mutations, further indicating that other epigenetic events may lead to Pten loss in some cases of HS (Table S1A and data not shown).

There exists an intimate relationship between PI3K/Akt and RAS-MAPK pathways, and the latter is similarly activated in a wide range of tumors (Sebolt-Leopold and Herrera, 2004). We observed an increase in phosphorylation of both ERK1 and ERK2 (p44 and p42) in several of the HS samples when compared both to normal tissues from wild-type mice and to lymphomas from $Ink4a/Arf^{-/-}$ mice. The expression level of ERK1 is also elevated in several of the HS samples (Figure 3B). Thus, in addition to increased signaling through the PI3K/Akt pathway, the RAS-MAPK pathway appears to be hyperactivated in HS, as evidenced by increased expression and phosphorylation of ERK. This biochemical finding recalls previous observations of occasional HS cases in pEμ-Ras transgenic mice (Haupt et al., 1992).

Cell biological and developmental impact of dual *Pten* and *Ink4a/Arf* inactivation in murine lymphoid and histiocytic cells

To understand better the role of *Pten* and *Ink4a/Arf* in the development of the aforementioned neoplastic phenotypes, we assessed the cellularity, proliferation, and apoptosis profiles of the lymphoid and histiocytic compartments in prelymphomatous wild-type and mutant samples (Figure 4, Figure S1, and Tables S2 and S3). Through 8 weeks of age, all mutant mice demonstrated progressive lymphoid organ enlargement and increased total cellularity in the spleen that was more severe in $Pten^{+/-}$ $Ink4a/Arf^{-/-}$ mice compared with single mutant and wild-type control littermates (Table S2). At 20 weeks of age, histologic surveys of lymph nodes, thymuses, and spleens of $Pten^{+/-}$ $Ink4a/Arf^{-/-}$, but not single mutant or wild-type mice, revealed significantly increased numbers of lymphatic follicles containing large irregularly shaped germinal centers in lymph nodes, prominent B cell infiltration of the thymic medulla, and increased white pulp areas with frequent, prominent germinal centers and marginal zone areas in the spleen (Figure 4). Moreover, flow cytometric analyses of thymuses revealed an expansion of $B220^+$ B cells relative to $CD3^+$ T cells in $Pten^{+/-}$ and $Pten^{+/-}$ $Ink4a/Arf^{-/-}$ mutant strains, suggesting that *Pten* haploinsufficiency is the primary driver of this B cell phenotype (Table S3 and data not shown). In contrast, the phenotype of frequent germinal centers appears to be related to the *Ink4a/Arf* deficiency as it is correlated with the $Ink4a/Arf^{-/-}$ mutant genotype and not *Pten* status (Figure 4).

Further assessment of peripheral B and T cells included mitogen stimulation assays of total lymph node mononuclear cells derived from the various genotypes. Relative to wild-type controls, $Pten^{+/-}$ and $Ink4a/Arf^{-/-}$ lymphoid cells showed increased proliferation upon exposure to the polyclonal B cell and macrophage activator LPS, or to the T cell activators CD3 and CD28 (Figure S1B), findings consistent with previous reports establishing a role of *Pten* and *Ink4a/Arf* in the control of lymphoid cell proliferation (Di Cristofano et al., 1999; Hoang-Xuan et al., 2001; Serrano et al., 1996; Suzuki et al., 2001, 2003). Compared with these single mutants, $Pten^{+/-}$ $Ink4a/Arf^{-/-}$ lymphoid cells exhibited increased mitogen-induced proliferation as measured by thymidine incorporation (Figure S1B). Analysis of apoptotic indices in prelymphomatous lymph nodes revealed significantly fewer apoptotic lymphoid cells in $Pten^{+/-}$ $Ink4a/Arf^{-/-}$ (39 per 10 HPF) and $Pten^{+/-}$ (38 per 10 HPF) samples compared to wild-type (70 per 10 HPF) or $Ink4a/Arf^{-/-}$ mice (65 per 10 HPF) (Figure S1C), observations consistent with previously reported roles of *Pten* in lymphoid survival (Podsypanina et al., 1999; Suzuki et al., 2001).

Since the macrophage lineage is the presumed origin of HS, this lineage was examined in the prelymphomatous tissues of the various genotypes. MAC2 antibody staining revealed significant expansion of the macrophage population in $Pten^{+/-}$ *Ink4a/*

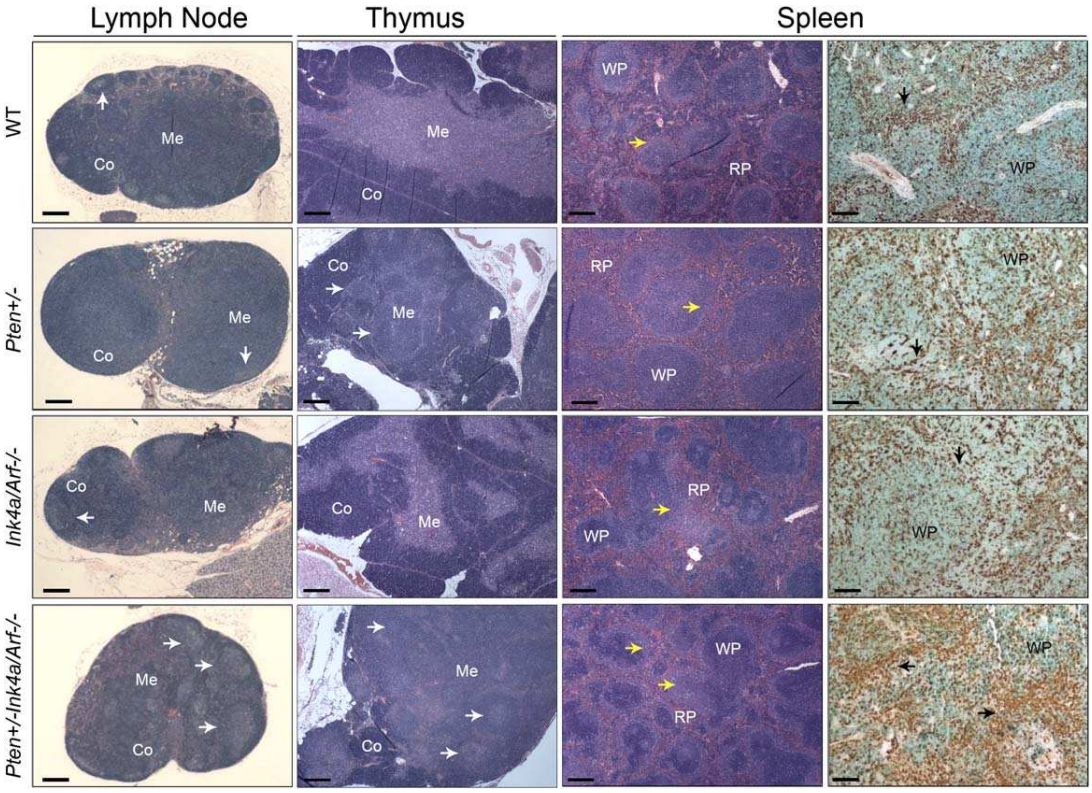

Figure 4. B cell and histiocytic hyperplasia

Lymphoid tissues from 20-week-old WT, *Pten*$^{+/-}$, *Ink4a/Arf*$^{-/-}$, and *Pten*$^{+/-}$ *Ink4a/Arf*$^{-/-}$ mice were analyzed by H&E staining and immunoperoxidase studies using MAC2 antibodies (far right column). Note frequent enlarged germinal centers (white arrows) in *Pten*$^{+/-}$ *Ink4a/Arf*$^{-/-}$ lymph node, thymic medulla, and splenic white pulp. Note extensive lymphoid infiltration of thymic medulla in *Pten*$^{+/-}$ and *Pten*$^{+/-}$ *Ink4a/Arf*$^{-/-}$ mice and expanded population of MAC2^{+} histiocytes (black arrows) in *Pten*$^{+/-}$ *Ink4a/Arf*$^{-/-}$ splenic marginal zones (yellow arrows). Me, medulla; Co, cortex; WP, white pulp; RP, red pulp. Scale bars: lymph node and thymus, 0.5 mm; spleen, 125 μm.

Arf$^{-/-}$ spleens relative to wild-type, *Pten*$^{+/-}$, and *Ink4a/Arf*$^{-/-}$ spleens, consistent with cooperative roles of *Pten* and *Ink4a/Arf* in restricting macrophage growth (Figure 4). Expansion of histiocytes was observed in other *Pten*$^{+/-}$ *Ink4a/Arf*$^{-/-}$ tissues, including the liver (data not shown). This result is particularly interesting in light of the recent observation highlighting the role of p16^{INK4a} and p19^{ARF} in immortalization of murine bone marrow-derived macrophages (Randle et al., 2001). As shown in Figure 5B, flow cytometric analysis of premalignant bone marrow mononuclear cells revealed an expanded population of mature myeloid and macrophages as well as a population of biphenotypic B220^{+}CD117^{+} cells in *Pten*$^{+/-}$ *Ink4a/Arf*$^{-/-}$ mice, but not in control and *Ink4a/Arf*$^{-/-}$ mice (Figure 5B), pointing to a role of *Pten* in controlling the proliferation and differentiation potential of a common myelolymphoid progenitor (Figures 5C and 5D).

PTEN, p16^{INK4A}, and p14^{ARF} are targeted in a subset of human HS

Our findings of significant expansion of macrophage populations and increased incidence of HS in *Pten*$^{+/-}$ *Ink4a/Arf*$^{-/-}$ mice prompted us to investigate the status of PTEN and p16^{INK4A} in human HS (Table 2 and Figure 6), a rare human neoplasm with only a limited number of cases reported in the world literature. Immunohistochemical analysis was performed using clinically standardized PTEN and p16^{INK4A} antibodies on a panel of ten archival cases of human HS (Hornick et al., 2004). Loss of immunoreactivity for either PTEN or p16^{INK4A} alone was seen in four and five cases, respectively. Three of the ten cases showed concomitant lack of immunostaining for both PTEN and p16^{INK4A}, while four of the ten cases showed intact staining for both proteins (Table 2, Figure 6A, and data not shown). The presence of reactivity in nonlesional tumor cells served as internal positive controls. We further analyzed the activation status of Akt proteins in human HS using clinically standardized p-Akt antibodies. Most human HS cases revealed increased levels of p-Akt in the histiocytic tumor cells, while in adjacent normal cells p-Akt was either barely detectable or not detected at all (Table 2 and Figure 6A). These results indicate that, in human HS, Akt phosphorylation is a general pathogenetic event and suggest that additional mechanisms besides PTEN inactivation can lead to Akt activation, including among others changes in Src activity, PTEN expression, PI3K activity, or receptor tyrosine kinase signaling (Hodgson et al., 2005; Lu et al., 2003; Nagata et al., 2004; Shekar et al., 2005; Wang et al., 2005). Nested PCR enabled further molecular investigations of laser-captured tumor cells for six of ten tumors (Table 2 and Figure 6B). Using specific oligonucleotides to amplify each of the nine exons of *PTEN* (Table S1), no amplification of exons 6 to 9 in tumor H3 was seen, nor amplification of all nine exons in tumor H6. These *PTEN* gene deletion patterns are not related to DNA quality

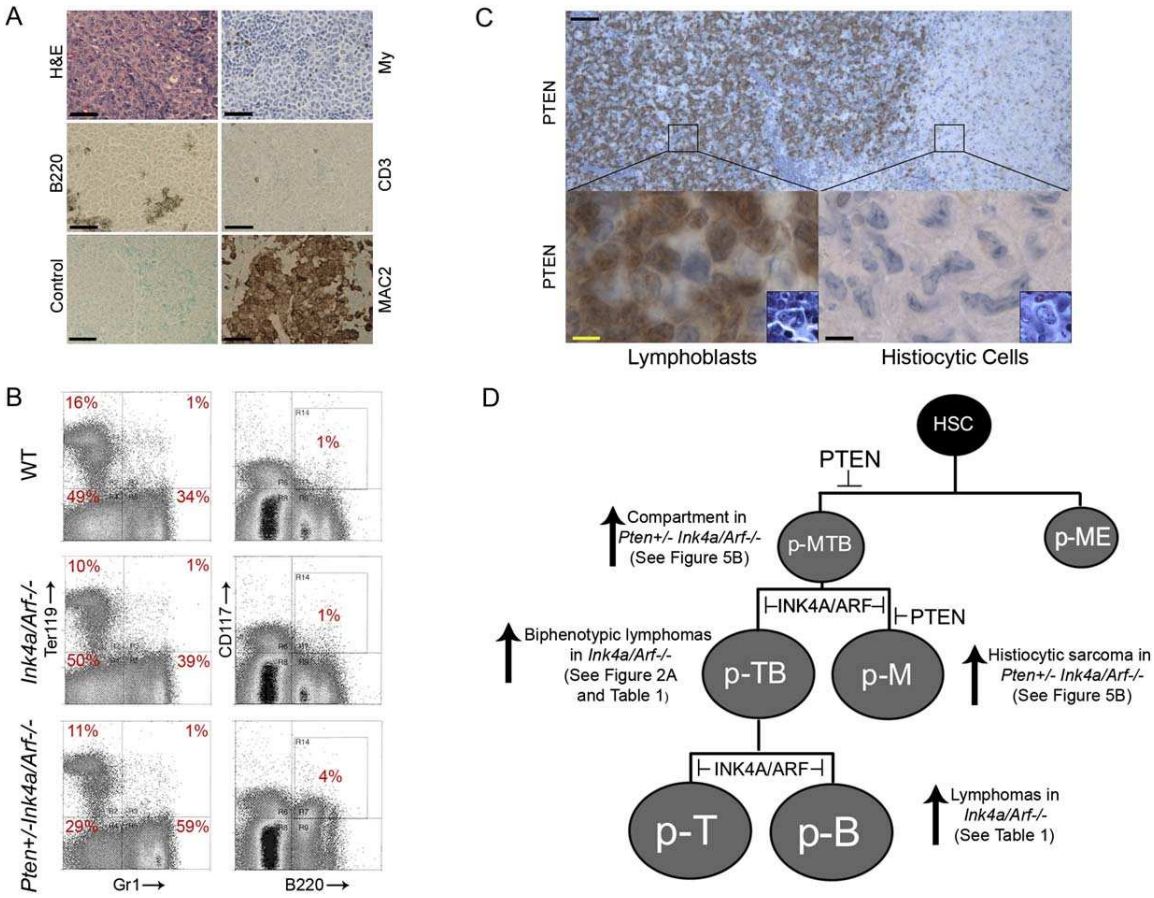

Figure 5. Proposed model for PTEN and INK4A/ARF function in hematopoiesis

A: Analysis of myeloperoxidase (My), B220, CD3, and MAC2 antibodies on paraffin-embedded tissue sections from mouse HS. Control stain without primary antibody. Scale bars, 50 μm.

B: Flow cytometric analysis of bone marrow mononuclear cells derived from mice. Note expanded populations of Gr-1$^+$ and B220$^+$CD117$^+$ cells in *Pten*$^{+/-}$ *Ink4a/Arf*$^{-/-}$ mice.

C: Analysis of PTEN expression in HS. Note presence of immunoreactivity in lymphoblastic cells but complete absence of reactivity in histiocytic cells. H&E inserts. Scale bars: upper panel, 125 μm; lower panel and inserts, 20 μm.

D: Proposed model for PTEN and INK4A/ARF function in hematopoiesis. Arrows indicates enhanced populations.

issues (see below) and concur with the lack of PTEN protein signals above (Table 2, Figure 6B, and data not shown). In the case of p16^{INK4A} and p14^{ARF}, all samples showed the presence of amplification products for all four coding exons, and these fragments were determined to be free of point mutations upon sequence analysis (Table 2, Figure 6B, and data not shown). In addition, TP53 immunohistochemistry revealed low or undetectable expression in six of nine human samples analyzed

Table 2. Human histiocytic sarcoma immunohistochemical and molecular analysis

Tumor	PTEN	p16^{INK4A}	p-Akt	TP53*	*PTEN* deletion	*p16^{INK4A}* promoter methylation	*p14^{ARF}* promoter methylation
H1	+++	+++	+++	++++	N	N	N
H2	–	–	+++	+	N	N	Y
H3	–	–	+++	++	Y	Y	Y
H4	+	+	ND	ND	N	N	Y
H5	–	+	++	+	N	N	Y
H6	–	–	++	+++	Y	Y	N
H7	+++	+++	+++	++	ND	N	Y
H8	–	++	++	++	ND	N	Y
H9	++	++	+++	+	ND	N	Y
H10	+	–	++	++++	ND	N	N

An arbitrary scale for grading immunohistochemical signal was used with ''++++'' as high expression and ''–'' as no expression. *For TP53 immunostains, a +++ value was assigned to control normal histiocytes. Molecular analysis of *PTEN* in H7–H10 was not determined (ND) due to insufficient DNA.

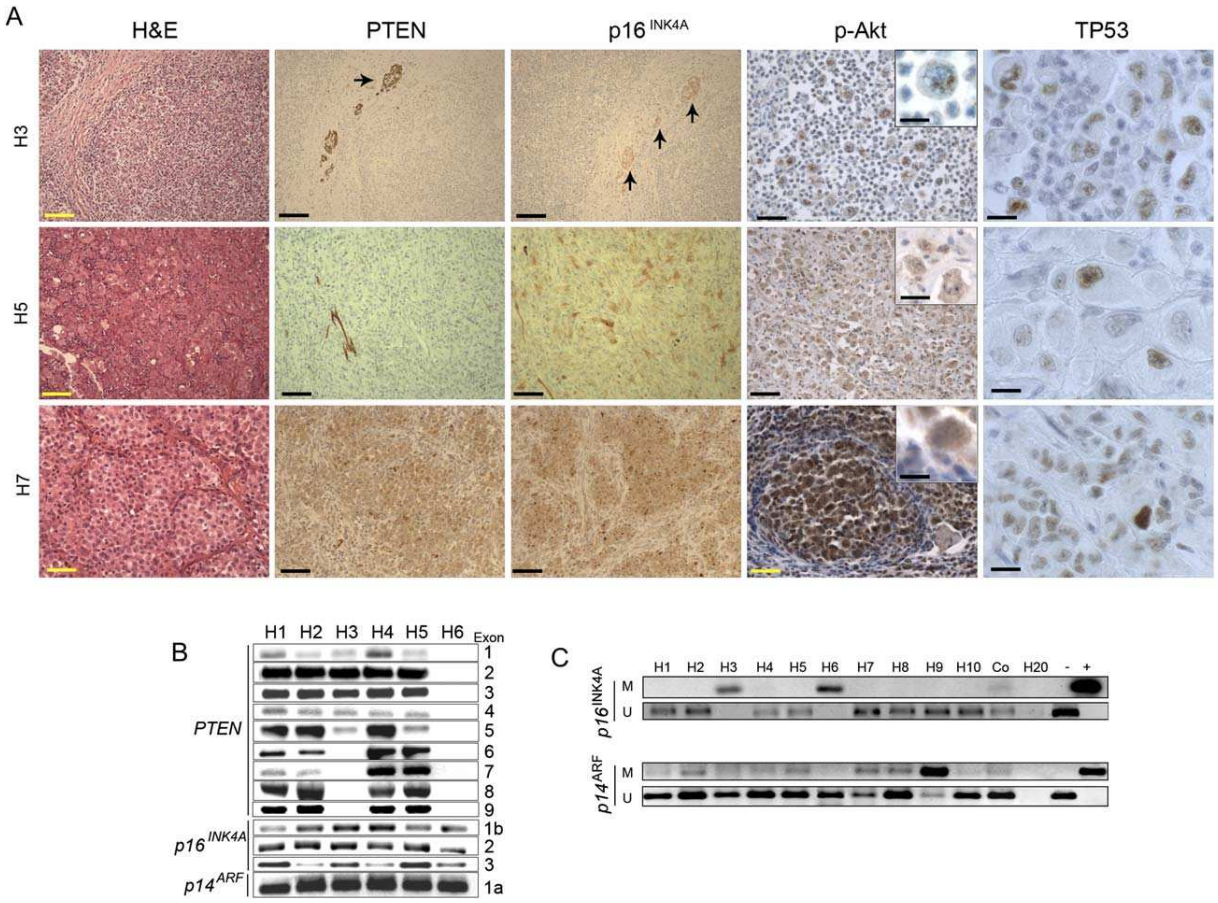

Figure 6. Immunohistochemistry and methylation analysis

A: Analysis of H&E, PTEN, $p16^{INK4A}$, p-Akt, and TP53 antibodies on paraffin-embedded tissue sections from human HS. Note lack of immunoreactivity of tumor cells for PTEN antibodies (H3 and H5) or $p16^{INK4A}$ antibodies (H5). Internal positive control, stromal cells (black arrows). Scale bars: H&E, PTEN, and $p16^{INK4A}$, 125 μm; p-Akt, 50 μm; TP53, 20 μm; inserts, 25 μm.

B: DNA was isolated from paraffin-embedded tissues and nested PCR-amplified products using a set of specific primers for each of nine exons of *PTEN* and each of four exons of $p16^{INK4A}/p14^{ARF}$. Note lack of PCR amplification of *PTEN* exons 6-9 in tumor H3 and exons 1-9 in tumor H6.

C: DNA from primary tumors was subjected to methylation-specific PCR amplification using methylated (M) or unmethylated (U) $p16^{INK4A}$- or $p14^{ARF}$-specific primer sets. Note the presence of PCR products using $p16^{INK4A}$- or $p14^{ARF}$-methylated primers from tumors H3 and H6 and H2, H4, H5, and H7–H9, respectively. Control male human DNA (Co); no DNA (H_2O); unmethylated DNA (−); Sss I (CpG) methylase-treated DNA (+).

(H2, H3, H5, H7–H9); moreover, sequence analysis did not detect any mutations in exons 5 to 9 in TP53 encoding sequence, including the two samples with moderate expression (Figure 6A, Table 2, Table S1, and data not shown). Finally, using methylation-specific PCR (MSP) (Esteller et al., 2001; Herman et al., 1996), $p16^{INK4A}$ promoter methylation was evident in two tumors (H3 and H6), while $p14^{ARF}$ promoter methylation was evident in seven of ten tumors (H2–H5, H7–H9). Very low levels or complete absence of $p14^{ARF}$ promoter methylation was observed in three tumors (H1, H6, and H10) (Figure 6C and Table 2). In agreement with the role of $p14^{ARF}$ in blocking MDM2-mediated degradation of p53 (Pomerantz et al., 1998; Zindy et al., 2003), the levels of $p14^{ARF}$ promoter methylation were inversely correlated with p53 immunoreactivity (Table 2). When using PCR oligos to detect unmethylated DNA promoter sequences, no PCR products were detected in the methylated positive control (Figure 6C). These molecular findings, coupled with genetic observations in the $Pten^{+/-}$ $Ink4a/Arf^{-/-}$ mice, support a model in which inactivation of PTEN, $p16^{INK4A}$, and $p14^{ARF}$ tumor suppressors and most likely their linked genetic elements are critical steps in the pathogenesis of human HS.

Discussion

In this study, we have investigated the genetic interactions of the *Pten* and *Ink4a/Arf* tumor suppressors in normal and neoplastic process in the hematopoietic system. These studies have revealed the presence of expanded populations of lymphocytes and histiocytes with a significant reduction in lymphoid tumor latency and a dramatic increase in the incidence of HS in compound *Pten and Ink4a/Arf* mutant mice. Correspondingly, analysis of the targeted lineages during the premalignant phase suggests that *Pten* and *Ink4a/Arf* mutations impact the control of proliferation and apoptosis, resulting in an expansion of the involved cell populations. Notably, consistent with the resultant neoplastic phenotypes, *Pten* and *Ink4a/Arf* were shown to serve

distinct and cooperative roles in hematopoietic lineage development with a notable expansion in mature B lymphocytes, granulocytes, and macrophages/histiocytes as well as biphenotypic $B220^{+}CD117^{+}$ cells in *Pten Ink4a/Arf* mutant mice. Importantly, the genetic and biochemical evidence of a cooperative role for *Pten* and *Ink4a/Arf* in constraining HS development translated to human HS wherein PTEN and $p16^{INK4A}$ were also found to be extinguished. Thus, murine modeling of disease has provided mechanistic insights into pathogenesis of human HS.

Deficiency of either *Pten* or *Ink4a/Arf* leads to B cell expansion, proliferation, and/or apoptotic defects of T cells (Figure 4, Figure S1, and Tables S2 and S3) (Di Cristofano et al., 1999; Kamijo et al., 1999; Podsypanina et al., 1999; Serrano et al., 1996; Sharpless et al., 2001, 2004; Suzuki et al., 2001, 2003). However, *Pten* and *Ink4a/Arf* appear to play cell-specific tumor suppressor roles in the hematopoietic system, as evidenced by markedly different tumor spectra. $Pten^{+/-}$ mice rarely develop lymphomas and instead sustain a lethal lymphoproliferative condition with histological and immunophenotypic features characteristic of certain autoimmune diseases (Figure 4) (Di Cristofano et al., 1999). Moreover, mice with B cell-specific homozygous deletion of *Pten* have a low incidence of lymphoma despite elevated levels of autoantibodies and a greatly increased B cell population (Suzuki et al., 2003). These observations are consistent with a critical role of *Pten* in the regulation of immune recognition (Di Cristofano et al., 1999) and B cell homeostasis but not in the suppression of B cell malignancy (Figure S1A) (Suzuki et al., 2003). On the other hand, the rare lymphomas that do arise in $Pten^{+/-}$ animals possess a T cell phenotype and show LOH of the *Pten* wild-type allele (Figure S1A) (Suzuki et al., 1998). In addition, T cell-specific deletion of *Pten* leads to the development of T cell lymphomas and defects in central and peripheral tolerance, linking autoimmunity and lymphomagenesis (Suzuki et al., 2001). Overall, these results indicate that the development of rare lymphomas and the onset of autoimmune disease in $Pten^{+/-}$ mice are primarily associated with an intrinsic defect in the T cell compartment or are secondary to impaired T cell/B cell interactions, which may lead to defects in central or peripheral tolerance. Hence, *Pten* has a cell type-specific tumor suppressor activity in the lymphoid compartment. In T cells, *Pten* appears to behave as a classic tumor suppressor, undergoing "two-hit" inactivation (Suzuki et al., 2001). In B cells, *Pten* haploinsufficiency or homozygous inactivation causes nonclonal B cell growth but does not lead to B cell lymphomas (Suzuki et al., 2003); rather, these data prompt speculation that *Pten* haploinsufficiency promotes immune dysfunction that facilitates lymphomagenesis in the T cell compartment.

Ink4a/Arf is required for suppression of both T and B cell malignancies (Table 1) (Kamijo et al., 1999; Kamijo et al., 1997; Serrano et al., 1996; Sharpless et al., 2001). Notably, despite the role of *Pten* in homeostasis of these compartments, *Pten* heterozygosity does not appear to strongly synergize with *Ink4a/Arf* deficiency in promoting T or B cell lymphomas. Instead, there is an increased incidence of HS bearing remarkable pathological similarity to the rare human disease (Table 1 and Figure 2B). These tumors are thought to arise from macrophage lineages, a compartment that is expanded in prelymphomatous $Pten^{+/-}$ $Ink4a/Arf^{-/-}$ mice (Figure 4). Of potential relevance, mice lacking $p19^{ARF}$ but expressing functional $p16^{INK4a}$ develop lymphomas, predominantly of T cell origin (Kamijo et al., 1999); however, when crossed to Bax deficient mice, a proportion (2 of 25) of *Arf* null animals developed HS (Eischen et al., 2002). The emergence of comparable tumor phenotypes in these models likely reflects disruption of common biochemical pathways. *Pten* and *Bax* deficiency may have overlapping roles in the genesis of HS, since *Pten* loss promotes activation of Bcl-xl and Bcl2, which are antiapoptotic antagonists of Bax (Huang et al., 2001). The *Ink4a/Arf* locus also appears to be of particular importance in macrophage biology, as evidenced by the requirement of dual *Ink4a* and *Arf* inactivation to enable immortalization of this lineage (Randle et al., 2001). Given these data and the very high penetrance of HS in our cohort harboring inactivation of both *Ink4a* and *Arf*, one might predict that $p16^{INK4a}$ may be inactivated in the $Arf^{-/-}$ $Bax^{-/-}$ tumors (Eischen et al., 2002).

Our results suggest that *Pten* and *Ink4a/Arf* are required at different stages during hematopoiesis and are consistent with a model of hematopoietic differentiation slightly different from the currently accepted model (Figure 5D) (M. Lu et al., 2002). INK4a/ARF appear to be primarily involved in controlling the proliferative and/or differentiation potential of a "common T and B cell lymphoid progenitor (p-TB)" and a minor role in a myelolymphoid progenitor (p-MTB) (Lacaud et al., 1998). Our data are also consistent with a model in which a functional *Pten* gene is required for the proper development of granulocytes and macrophages from a myelolymphoid progenitor (p-MTB) (Figure 5D). The fact that erythroid lineage neoplasms have not been identified in $Pten^{+/-}$, $Ink4a/Arf^{-/-}$, or $Pten^{+/-}$ $Ink4a/Arf^{-/-}$ mice is consistent with a lack of role for Pten and INK4a/ARF at the level of pluripotent hematopoietic stem cells (HSCs). The development of biphenotypic lymphomas with cells expressing both T and B cell differentiation markers but not myeloid and histiocytic markers in $Ink4a/Arf^{-/-}$ mice suggest the existence of a common T and B cell progenitor (p-TB) which is dependent on INK4a/ARF in restricting proliferation and/or differentiation toward B or T lymphocytes (Figure 5D). The development of HS at low frequency in $Ink4a/Arf^{-/-}$ is also consistent with a minor role of INK4a/ARF in restricting differentiation of the p-MTB progenitor toward myeloid cells and histiocytes (p-M). In addition, the marked increase in HS, but no change in total numbers of T and B cell neoplasms in $Pten^{+/-}$ $Ink4a/Arf^{-/-}$ mice as compared with $Ink4a/Arf^{-/-}$ mice, and the presence of expanded populations of biphenotypic $B220^{+}CD117^{+}$ myelolymphoid cells in $Pten^{+/-}$ $Ink4a/Arf^{-/-}$ but not in $Ink4a/Arf^{-/-}$ mice point to a role of Pten in restricting differentiation of the p-MTB toward histiocytes and myeloid cells. These results document overlapping and nonoverlapping roles of PTEN and INK4A/ARF in the process of hematopoietic diversification, support the existence of myelolymphoid progenitor (p-MTB), and suggest the existence of a common T and B cell progenitor (p-TB), which may explain the rare occurrence of acute leukemia of ambiguous lineage or biphenotypic acute leukemias in the clinical practice (Brunning, 2003).

Previous studies have documented the development of hamartoma-like, hyperplastic-dysplastic changes in the prostate, skin, and colon of $Pten^{+/-}$ mice, and these changes appear to be associated with retention of the remaining allele of *Pten* (Di Cristofano et al., 1998). In our studies, $Pten^{+/-}$ mice did not show any evidence of histiocytic hyperplasia, which was only detected in young, pre-HS $Pten^{+/-}$ $Ink4a/Arf^{-/-}$ mice, supporting the idea that certain compartments such as the myelolymphoid and histiocytic compartments are less affected by Pten

dose reduction and require the addition of $p16^{INK4a}$ or $p19^{ARF}$ deficiency to elicit a neoplastic phenotype. Contrary to pre-HS *Pten*$^{+/-}$ *Ink4A/Arf*$^{-/-}$ mice, almost all mouse HS cases analyzed showed LOH for *Pten*, indicating that full HS development in mice commonly occurs in the complete absence of Pten. Therefore, it seems plausible that the expansion of myelolymphoid precursors in the setting of *Pten* heterozygosity and *Ink4a/Arf* nullizygosity generates a pool of cells at risk for additional transforming events.

Additional insights into the basis for the cooperative interactions between *Pten* and *Ink4a/Arf* derive from proviral insertional mutagenesis studies in *Ink4a/Arf*$^{-/-}$ mice (Lund et al., 2002). In that study, 80% of *Ink4a/Arf*$^{-/-}$ mice infected with Moloney murine leukemia virus (MoMuLV) developed lymphomas, and approximately 55% of these mice also developed HS. While the *Pten* was not targeted for proviral insertional inactivation, there were numerous events targeting components of the PI3K pathway (Lund et al., 2002). Remarkably, three retroviral insertions target phosphatase genes. The *Ptpn1* and *Hcph* genes have been proposed to activate Src through removal of an inhibitory tyrosine phosphate within the Src-homology 2 (SH2) domain. Importantly, in the context of PI3K pathway, activation of Src is known to inactivate PTEN via phosphorylation (Lu et al., 2003; Nagata et al., 2004). The other insertion targeted the *Dusp5* gene encoding a dual-specificity protein phosphatase, which is thought to negatively regulate the activity of the ERK1 MAP kinase (Ishibashi et al., 1994) and consistent with the known links between the RAS-MAPK and PI3K pathways (Pandey et al., 1999).

On the molecular level, a proportion of the HS cases in our cohort lost the wild-type Pten allele. These changes were associated with aberrant activation of the PI3K/Akt signaling pathway as well as the RAS-MAPK pathway, as evidenced by increased levels in phosphorylation of Akt and both ERK 1 and ERK 2 (p44 and p42). In humans, HS is a rare malignant proliferation of cells showing morphologic and immunophenotypic features similar to those of mature tissue histiocytes. This neoplasm is typically very aggressive and poorly responsive to existing therapy and is of unknown molecular etiology (Banks and Warnke, 2001; Hornick et al., 2004). The resemblance between the phenotype and the clinical behavior of the neoplasms arising in *Pten*$^{+/-}$ *Ink/Arf*$^{-/-}$ mice and HS in humans is consistent with cooperative roles of PTEN and INK4A/ARF tumor suppressors or linked genetic elements in the pathogenesis of this poorly understood human condition. Further corroboration of this genetic interaction was secured in translational studies documenting PTEN, $p16^{INK4A}$, and $p14^{ARF}$ loss by deletion of *PTEN* genomic sequences and *p16*^{INK4A} and/or *p14*^{ARF} promoter region hypermethylation in a subset of tumors, while Akt activation appeared as a common mechanism detected in most human tumors. These results suggest molecular heterogeneity of human HS and many putative mechanisms leading to Akt activation, and we cannot exclude the possibility that the human disease comprises distinct human HS subsets that are not distinguished by current morphological and marker criteria. In the remaining samples with intact PTEN and $p16^{INK4A}$ expression, it is reasonable to assume that other components of the p16-Rb, Arf-p53, and PI3K-PTEN pathways are targeted as suggested by the occurrence of HS in the *Arf*$^{-/-}$ *Bax*$^{-/-}$ model and the MoMuLv mutagenesis studies in *Ink4a/Arf*$^{-/-}$ mice. Based upon the genetic and biochemical findings of our study, we propose that emerging PI3K, RAS/MAPK, and cdk4/6 inhibitors may provide effective targeted therapies for this currently intractable disease.

Experimental procedures

Mutant mice

Pten and *Ink4a/Arf* mutant mice were produced as described elsewhere (Podsypanina et al., 1999; Serrano et al., 1996) and maintained on a mixed FVB/nC57BL/6 background. Mice heterozygous for *Pten* and *Ink4a/Arf* mutant alleles were intercrossed to generate all of the genotypes analyzed in this study and maintained on a mixed FVB/nC57BL/6 background. During an observation period of 60 weeks, all wild-type control littermates remained tumor free. All animal experiments were approved by and conform to the standards of the Institutional Animal Care and Use Committee at the Dana-Farber Cancer Institute.

Histology, TUNEL assay, immunohistochemistry, and flow cytometry

Formalin-fixed tissues were embedded in paraffin, sectioned, and stained with H&E. Apoptotic cells were detected with the Apoptag assay from Intergen. Tissue sections were incubated with 5 μg/ml of primary antibodies or a corresponding IgG fraction of preimmune serum in 3% BSA-PBS blocking solution for 16 hr at 4°C. Anti-mouse MAC2 monoclonal antibody was obtained from Cedarlane. Anti-mouse CD45R (clone RA3-6B2) was obtained from Pharmingen. Anti-human CD3 (MCA1477) and anti-mouse F4/80 (MCAP497) antibodies were obtained from Serotec. Anti-mouse Bcl-6 (N-3) antibody was obtained from Santa Cruz Biotechnology. Anti-PTEN (clone 6H2.1) was from Cascade Bioscience. Primary antibodies were visualized with the corresponding biotinylated antibody coupled to streptavidin-peroxidase complex from Vector Labs. Flow cytometry was done using a Coulter Epics Profile II flow cytometer and cell sorter. Lymphoid cells were prepared according to standard procedures, and 10^6 cells per reaction were incubated with antibodies for 30 min on ice and resuspended in 500 μl of 2% paraformaldehyde. Anti-mouse CD3 (145-2C11), CD4 (L3T4), CD8 (Ly-2), CD45R/B220 (RA3-6B2), IgM, Mac-1, CD117 (2b8), Gr-1 (RB6-8C5), and p16 (clone G175-405) antibodies were from Pharmingen.

In vitro proliferation assays

Total single cell suspensions from 6- to 8-week-old lymph nodes were prepared according to standard procedures, and 2×10^5 cells were plated in triplicate in 96-well plates and stimulated with LPS (20 μg/ml) or CD3 (10 μg/ml) with CD28. After 48 hr of stimulation, the cells were pulsed with [^{3}H] thymidine for the final 16 hr of growth, and incorporated [^{3}H] thymidine was measured. Results are expressed as the arithmetic mean ± SD of triplicate cultures. Similar results were obtained in three independent experiments.

Western blotting analysis

Whole-cell extracts from 6- to 8-week-old mouse single cell suspensions of lymph node cells or snap-frozen lymphomas were prepared in the presence of 1 mM orthovanadate, 5 mM NaF, and protease inhibitors. Samples were mixed with 4× NuPAGE loading buffer containing 50 mM DTT and heated at 70°C for 10 min before being loaded into 5%–12% Bis-Tris NuPAGE gels. Proteins were transferred to nitrocellulose membranes, blocked in TBS containing 0.1% Tween 20 and 5% nonfat milk, and incubated overnight at 4°C with primary antibodies. Rabbit monoclonal p-Akt (T308 and S473), rabbit polyclonal total Akt, p-ERK1/2 (T202/Y204), and total ERK1/2 antibodies were from Cell Signaling Technology. Anti-PTEN (HRP-conjugated A2B1) was from Santa Cruz, and the β-Actin antibody, used as a loading control, was a gift from Don Cleveland (LICR, University of California, San Diego). HRP-linked anti-mouse and anti-rabbit were used for secondary antibodies.

Southern blot analysis

Genomic DNA was isolated by the Puregene DNA isolation system (Gentra Systems). Southern blot analysis for the loss of *Pten* gene was done as described elsewhere (You et al., 2002). For the T cell receptor gene rearrangement studies, the DNA was digested with BglII restriction enzyme, and as a radiolabel probe, a 1.6 BamHI-KpnI genomic fragment downstream and adjacent to the mouse TCR Jβ1 gene segment was used. For the B cell receptor gene rearrangement studies, the DNA was digested with EcoRI

restriction enzyme and as a radiolabeled probe; a 1.9 BamHI-EcoRI genomic fragment downstream and adjacent to the mouse heavy chain locus JH segment was used.

Laser capture microdissection, DNA preparation, bisulfite modification, PCR amplification, and genomic sequencing

Laser capture microdissection (LCM) was performed on H&E-stained slides. Histiocytes were microdissected using the PixCell II Laser Capture Microdissection System (Arcturus Bioscience). About 5000 cells were digested with 1 mg/ml proteinase K at 37ºC for 16 hr and then heated at 94ºC for 10 min. One microliter of the supernatant was used as template for nested PCR using specific primer pairs (Table S1), and the PCR products were subjected to both agarose electrophoresis and sequencing. LCM was repeated for all specimens to verify the results. The remaining DNA was subjected to bisulfite modification as described (Herman et al., 1996) and used for methylation-specific PCR of $p16^{INK4A}$ (Herman and Baylin, 2003) and $p14^{ARF}$ (Esteller et al., 2001) promoter sequences (Table S1).

Supplemental data

The Supplemental Data include one supplemental figure and three supplemental tables and can be found with this article online at http://www.cancercell.org/cgi/content/full/9/5/379/DC1/.

Acknowledgments

We wish to thank N. Bardeesy, G. Tonon, R.A. Aguirre, R. Kollipara, and E. Farazi for valuable comments on the manuscript; Robert Bachoo for providing $Pten^{-/-}$ cells; and Ilana Perna for technical assistance. R.A.D. is an American Cancer Society Research Professor and an Ellison Medical Foundation Senior Scholar. This work was supported by the Bennett LeBow Fund to Cure Myeloma (R.A.D.), NIH grants P01 CA95616 (R.A.D., F.B.F., and W.K.C.), and U01 CA84313 (R.A.D.). W.K.C. is a Fellow of the National Foundation for Cancer Research, and F.B.F. is partially supported by the Goldhirsh Foundation. D.R.C. is supported by a Mentored Clinician Scientist Award (K08AG0103) and is a Sidney Kimmel Foundation Scholar.

Received: November 27, 2005
Revised: February 17, 2006
Accepted: March 10, 2006
Published: May 15, 2006

References

Banks, P., and Warnke, R. (2001). Chapter 10: Histiocytic and Dendritic Cell Neoplasms. In World Health Organization Classification of Tumours: Pathology and Genetics of Tumours of Hematopoetic and Lymphoid Tissues, E. Jaffe, N.L. Harris, H. Stein, and J.W. Vardiman, eds. (Lyon, France: IARC Press), pp. 189–280.

Brunning, R.D. (2003). Classification of acute leukemias. Semin. Diagn. Pathol. *20*, 142–153.

Burri, N., Shaw, P., Bouzourene, H., Sordat, I., Sordat, B., Gillet, M., Schorderet, D., Bosman, F.T., and Chaubert, P. (2001). Methylation silencing and mutations of the p14ARF and p16INK4a genes in colon cancer. Lab. Invest. *81*, 217–229.

Cantley, L.C., and Neel, B.G. (1999). New insights into tumor suppression: PTEN suppresses tumor formation by restraining the phosphoinositide 3-kinase/AKT pathway. Proc. Natl. Acad. Sci. USA *96*, 4240–4245.

Cline, M.J. (1994). Histiocytes and histiocytosis. Blood *84*, 2840–2853.

Di Cristofano, A., Pesce, B., Cordon-Cardo, C., and Pandolfi, P.P. (1998). Pten is essential for embryonic development and tumour suppression. Nat. Genet. *19*, 348–355.

Di Cristofano, A., Kotsi, P., Peng, Y.F., Cordon-Cardo, C., Elkon, K.B., and Pandolfi, P.P. (1999). Impaired Fas response and autoimmunity in Pten+/− mice. Science *285*, 2122–2125.

Eischen, C.M., Rehg, J.E., Korsmeyer, S.J., and Cleveland, J.L. (2002). Loss of Bax alters tumor spectrum and tumor numbers in ARF-deficient mice. Cancer Res. *62*, 2184–2191.

Esteller, M., Cordon-Cardo, C., Corn, P.G., Meltzer, S.J., Pohar, K.S., Watkins, D.N., Capella, G., Peinado, M.A., Matias-Guiu, X., Prat, J., et al. (2001). p14ARF silencing by promoter hypermethylation mediates abnormal intracellular localization of MDM2. Cancer Res. *61*, 2816–2821.

Haupt, Y., Harris, A.W., and Adams, J.M. (1992). Retroviral infection accelerates T lymphomagenesis in E mu-N-ras transgenic mice by activating c-myc or N-myc. Oncogene *7*, 981–986.

Herman, J.G., and Baylin, S.B. (2003). Gene silencing in cancer in association with promoter hypermethylation. N. Engl. J. Med. *349*, 2042–2054.

Herman, J.G., Graff, J.R., Myohanen, S., Nelkin, B.D., and Baylin, S.B. (1996). Methylation-specific PCR: a novel PCR assay for methylation status of CpG islands. Proc. Natl. Acad. Sci. USA *93*, 9821–9826.

Hoang-Xuan, K., He, J., Huguet, S., Mokhtari, K., Marie, Y., Kujas, M., Leuraud, P., Capelle, L., Delattre, J.Y., Poirier, J., et al. (2001). Molecular heterogeneity of oligodendrogliomas suggests alternative pathways in tumor progression. Neurology *57*, 1278–1281.

Hodgson, J.G., Malek, T., Bornstein, S., Hariono, S., Ginzinger, D.G., Muller, W.J., and Gray, J.W. (2005). Copy number aberrations in mouse breast tumors reveal loci and genes important in tumorigenic receptor tyrosine kinase signaling. Cancer Res. *65*, 9695–9704.

Hornick, J.L., Jaffe, E.S., and Fletcher, C.D. (2004). Extranodal histiocytic sarcoma: clinicopathologic analysis of 14 cases of a rare epithelioid malignancy. Am. J. Surg. Pathol. *28*, 1133–1144.

Huang, H., Cheville, J.C., Pan, Y., Roche, P.C., Schmidt, L.J., and Tindall, D.J. (2001). PTEN induces chemosensitivity in PTEN-mutated prostate cancer cells by suppression of Bcl-2 expression. J. Biol. Chem. *276*, 38830–38836.

Ishibashi, T., Bottaro, D.P., Michieli, P., Kelley, C.A., and Aaronson, S.A. (1994). A novel dual specificity phosphatase induced by serum stimulation and heat shock. J. Biol. Chem. *269*, 29897–29902.

Kamijo, T., Zindy, F., Roussel, M.F., Quelle, D.E., Downing, J.R., Ashmun, R.A., Grosveld, G., and Sherr, C.J. (1997). Tumor suppression at the mouse INK4a locus mediated by the alternative reading frame product p19ARF. Cell *91*, 649–659.

Kamijo, T., Bodner, S., van de Kamp, E., Randle, D.H., and Sherr, C.J. (1999). Tumor spectrum in ARF-deficient mice. Cancer Res. *59*, 2217–2222.

Krimpenfort, P., Quon, K.C., Mooi, W.J., Loonstra, A., and Berns, A. (2001). Loss of p16Ink4a confers susceptibility to metastatic melanoma in mice. Nature *413*, 83–86.

Krishnamurthy, J., Torrice, C., Ramsey, M.R., Kovalev, G.I., Al-Regaiey, K., Su, L., and Sharpless, N.E. (2004). Ink4a/Arf expression is a biomarker of aging. J. Clin. Invest. *114*, 1299–1307.

Lacaud, G., Carlsson, L., and Keller, G. (1998). Identification of a fetal hematopoietic precursor with B cell, T cell, and macrophage potential. Immunity *9*, 827–838.

Li, J., Yen, C., Liaw, D., Podsypanina, K., Bose, S., Wang, S.I., Puc, J., Miliaresis, C., Rodgers, L., McCombie, R., et al. (1997). PTEN, a putative protein tyrosine phosphatase gene mutated in human brain, breast, and prostate cancer. Science *275*, 1943–1947.

Lu, M., Kawamoto, H., Katsube, Y., Ikawa, T., and Katsura, Y. (2002). The common myelolymphoid progenitor: a key intermediate stage in hemopoiesis generating T and B cells. J. Immunol. *169*, 3519–3525.

Lu, Y., Yu, Q., Liu, J.H., Zhang, J., Wang, H., Koul, D., McMurray, J.S., Fang, X., Yung, W.K., Siminovitch, K.A., and Mills, G.B. (2003). Src family protein-tyrosine kinases alter the function of PTEN to regulate phosphatidylinositol 3-kinase/AKT cascades. J. Biol. Chem. *278*, 40057–40066.

Lund, A.H., Turner, G., Trubetskoy, A., Verhoeven, E., Wientjens, E., Hulsman, D., Russell, R., DePinho, R.A., Lenz, J., and van Lohuizen, M. (2002). Genome-wide retroviral insertional tagging of genes involved in cancer in Cdkn2a-deficient mice. Nat. Genet. *32*, 160–165.

Morse, H.C., III, Anver, M.R., Fredrickson, T.N., Haines, D.C., Harris, A.W., Harris, N.L., Jaffe, E.S., Kogan, S.C., MacLennan, I.C., Pattengale, P.K., and Ward, J.M. (2002). Bethesda proposals for classification of lymphoid neoplasms in mice. Blood *100*, 246–258.

Nagata, Y., Lan, K.H., Zhou, X., Tan, M., Esteva, F.J., Sahin, A.A., Klos, K.S., Li, P., Monia, B.P., Nguyen, N.T., et al. (2004). PTEN activation contributes to tumor inhibition by trastuzumab, and loss of PTEN predicts trastuzumab resistance in patients. Cancer Cell *6*, 117–127.

Pandey, S.K., Theberge, J.F., Bernier, M., and Srivastava, A.K. (1999). Phosphatidylinositol 3-kinase requirement in activation of the ras/C-raf-1/MEK/ERK and p70(s6k) signaling cascade by the insulinomimetic agent vanadyl sulfate. Biochemistry *38*, 14667–14675.

Podsypanina, K., Ellenson, L.H., Nemes, A., Gu, J., Tamura, M., Yamada, K.M., Cordon-Cardo, C., Catoretti, G., Fisher, P.E., and Parsons, R. (1999). Mutation of Pten/Mmac1 in mice causes neoplasia in multiple organ systems. Proc. Natl. Acad. Sci. USA *96*, 1563–1568.

Pomerantz, J., Schreiber-Agus, N., Liegeois, N.J., Silverman, A., Alland, L., Chin, L., Potes, J., Chen, K., Orlow, I., Lee, H.W., et al. (1998). The Ink4a tumor suppressor gene product, p19Arf, interacts with MDM2 and neutralizes MDM2's inhibition of p53. Cell *92*, 713–723.

Quelle, D.E., Zindy, F., Ashmun, R.A., and Sherr, C.J. (1995). Alternative reading frames of the INK4a tumor suppressor gene encode two unrelated proteins capable of inducing cell cycle arrest. Cell *83*, 993–1000.

Randle, D.H., Zindy, F., Sherr, C.J., and Roussel, M.F. (2001). Differential effects of p19(Arf) and p16(Ink4a) loss on senescence of murine bone marrow-derived preB cells and macrophages. Proc. Natl. Acad. Sci. USA *98*, 9654–9659.

Ruas, M., and Peters, G. (1998). The p16INK4a/CDKN2A tumor suppressor and its relatives. Biochim. Biophys. Acta *1378*, F115–F177.

Sakai, A., Thieblemont, C., Wellmann, A., Jaffe, E.S., and Raffeld, M. (1998). PTEN gene alterations in lymphoid neoplasms. Blood *92*, 3410–3415.

Sebolt-Leopold, J.S., and Herrera, R. (2004). Targeting the mitogen-activated protein kinase cascade to treat cancer. Nat. Rev. Cancer *4*, 937–947.

Serrano, M., Lee, H., Chin, L., Cordon-Cardo, C., Beach, D., and DePinho, R.A. (1996). Role of the INK4a locus in tumor suppression and cell mortality. Cell *85*, 27–37.

Sharpless, N.E., and DePinho, R.A. (1999). The INK4A/ARF locus and its two gene products. Curr. Opin. Genet. Dev. *9*, 22–30.

Sharpless, N.E., Bardeesy, N., Lee, K.H., Carrasco, D., Castrillon, D.H., Aguirre, A.J., Wu, E.A., Horner, J.W., and DePinho, R.A. (2001). Loss of p16Ink4a with retention of p19Arf predisposes mice to tumorigenesis. Nature *413*, 86–91.

Sharpless, N.E., Ramsey, M.R., Balasubramanian, P., Castrillon, D.H., and DePinho, R.A. (2004). The differential impact of p16(INK4a) or p19(ARF) deficiency on cell growth and tumorigenesis. Oncogene *23*, 379–385.

Shekar, S.C., Wu, H., Fu, Z., Yip, S.C., Nagajyothi, Cahill, S.M., Girvin, M.E., and Backer, J.M. (2005). Mechanism of constitutive phosphoinositide 3-kinase activation by oncogenic mutants of the p85 regulatory subunit. J. Biol. Chem. *280*, 27850–27855.

Simpson, L., and Parsons, R. (2001). PTEN: life as a tumor suppressor. Exp. Cell Res. *264*, 29–41.

Stanger, B.Z., Stiles, B., Lauwers, G.Y., Bardeesy, N., Mendoza, M., Wang, Y., Greenwood, A., Cheng, K.H., McLaughlin, M., Brown, D., et al. (2005). Pten constrains centroacinar cell expansion and malignant transformation in the pancreas. Cancer Cell *8*, 185–195.

Steck, P.A., Pershouse, M.A., Jasser, S.A., Yung, W.K., Lin, H., Ligon, A.H., Langford, L.A., Baumgard, M.L., Hattier, T., Davis, T., et al. (1997). Identification of a candidate tumour suppressor gene, MMAC1, at chromosome 10q23.3 that is mutated in multiple advanced cancers. Nat. Genet. *15*, 356–362.

Stepanova, L., and Sorrentino, B.P. (2005). A limited role for p16Ink4a and p19Arf in the loss of hematopoietic stem cells during proliferative stress. Blood *106*, 827–832.

Suzuki, A., de la Pompa, J.L., Stambolic, V., Elia, A.J., Sasaki, T., del Barco Barrantes, I., Ho, A., Wakeham, A., Itie, A., Khoo, W., et al. (1998). High cancer susceptibility and embryonic lethality associated with mutation of the PTEN tumor suppressor gene in mice. Curr. Biol. *8*, 1169–1178.

Suzuki, A., Yamaguchi, M.T., Ohteki, T., Sasaki, T., Kaisho, T., Kimura, Y., Yoshida, R., Wakeham, A., Higuchi, T., Fukumoto, M., et al. (2001). T cell-specific loss of Pten leads to defects in central and peripheral tolerance. Immunity *14*, 523–534.

Suzuki, A., Kaisho, T., Ohishi, M., Tsukio-Yamaguchi, M., Tsubata, T., Koni, P.A., Sasaki, T., Mak, T.W., and Nakano, T. (2003). Critical roles of Pten in B cell homeostasis and immunoglobulin class switch recombination. J. Exp. Med. *197*, 657–667.

Vanhaesebroeck, B., and Alessi, D.R. (2000). The PI3K-PDK1 connection: more than just a road to PKB. Biochem. J. *346*, 561–576.

Wang, J., Ouyang, W., Li, J., Wei, L., Ma, Q., Zhang, Z., Tong, Q., He, J., and Huang, C. (2005). Loss of tumor suppressor p53 decreases PTEN expression and enhances signaling pathways leading to activation of activator protein 1 and nuclear factor kappaB induced by UV radiation. Cancer Res. *65*, 6601–6611.

Weiss, L.M. (2001). Histiocytic Sarcoma, Volume 1, Second Edition (Lyon, France: IARC Press).

You, M.J., Castrillon, D.H., Bastian, B.C., O'Hagan, R.C., Bosenberg, M.W., Parsons, R., Chin, L., and DePinho, R.A. (2002). Genetic analysis of Pten and Ink4a/Arf interactions in the suppression of tumorigenesis in mice. Proc. Natl. Acad. Sci. USA *99*, 1455–1460.

Zindy, F., Williams, R.T., Baudino, T.A., Rehg, J.E., Skapek, S.X., Cleveland, J.L., Roussel, M.F., and Sherr, C.J. (2003). Arf tumor suppressor promoter monitors latent oncogenic signals in vivo. Proc. Natl. Acad. Sci. USA *100*, 15930–15935.